Three-level all-fiber laser at 915 nm based on polarization-maintaining Nd^{3+}-doped silica fiber

Yafei Wang (王亚飞)[1], Xingyu Li (李星宇)[1], Jiamin Wu (吴佳民)[1], Xiulin Peng (彭秀林)[1], Jiangkun Cao (曹江坤)[1], Changsheng Yang (杨昌盛)[1], Shanhui Xu (徐善辉)[1,2], Zhongmin Yang (杨中民)[1], and Mingying Peng (彭明营)[1,2,*]

[1]State Key Laboratory of Luminescent Materials and Devices, Guangdong Provincial Key Laboratory of Fiber Laser Materials and Applied Techniques, Guangdong Engineering Technology Research and Development Center of Special Optical Fiber Materials and Devices, School of Materials Science and Technology, South China University of Technology, Guangzhou 510640, China

[2]Guangdong Engineering Technology Research and Development Center of High-performance Fiber Laser Techniques and Equipments, Zhuhai 519031, China

**Corresponding author: pengmingying@scut.edu.cn*

Received July 25, 2019; accepted September 20, 2019; posted online December 6, 2019

Nd^{3+}-doped fiber lasers at around 900 nm based on the $^4F_{3/2} \rightarrow {}^4I_{9/2}$ transition have obtained much research attention since they can be used as the laser sources for generating pure blue fiber lasers through the frequency doubling. Here, an all-fiber laser at 915 nm was realized by polarization-maintaining Nd^{3+}-doped silica fiber. A net gain per unit length of up to 1.0 dB/cm at 915 nm was obtained from a 4.5 cm fiber, which to our best knowledge is the highest gain coefficient reported in this kind of silica fiber. The optical-to-optical conversion efficiency varies with the active fiber length and the reflectivity of the output fiber Bragg grating (FBG), presenting an optimal value of 5.3% at 5.1 cm fiber length and 70% reflectivity of the low reflection FBG. Additionally, the linear distributed Bragg reflector short cavity was constructed to explore its potential in realizing single-frequency 915 nm fiber laser. The measurement result of longitudinal-mode properties shows it is still multi-longitudinal mode laser operation with 40 mm laser cavity. These results indicate that the Nd^{3+}-doped silica fiber could be used to realize all-fiber laser at 915 nm, which presents potential to be the seed source of high-power fiber laser.

Keywords: fiber laser; laser materials; neodymium.
doi: 10.3788/COL202018.011401.

Blue lasers have been attracting much attention due to their potential application in laser display, underwater communication, and the next-generation laser driven solid lighting[1–5]. Currently, the blue laser devices are principally based on commercial semiconductor laser diodes (LDs) that suffer from poor beam quality[5,6]. In order to obtain high performance blue laser sources, blue fiber lasers have obtained a lot of research attention because of their advantages in terms of the linewidth, noise, stability, beam quality, and compactness of device[3,7,8]. The current effective approach of realizing blue fiber lasers is through the nonlinear frequency doubling by efficient near-infrared (NIR) Yb^{3+}-doped fiber lasers. Yet, only blue-green fiber lasers at around 490 nm can be achieved by 980 nm Yb^{3+}-doped fiber due to the f-f transition nature of rare earth energy levels[7,9–13]. From the perspective of application, for instance, in the field of laser lighting, to match the absorption of the Ce:YAG converter and improve efficiency, fiber lasers in the pure blue region (450 nm) are required, which need a shorter NIR fiber laser[14,15]. For that sake, Nd^{3+}-doped fiber lasers based on three-level $^4F_{3/2} \rightarrow {}^4I_{9/2}$ transition near 900 nm appear as a more ideal choice[16–22]. The main issue of this three-level laser operation is the serious competition with the four-level $^4F_{3/2} \rightarrow {}^4I_{11/2}$ transition when pumped at 808 nm. The J-O theory analysis shows that this band is at a disadvantage in competition because its branching ratio (0.3) is lower than that (0.5) of the four-level transition[23,24]. Up to now, several strategies have been proposed to suppress the strong competition between these two transitions, such as cooling active fiber by liquid nitrogen, using the specially designed fiber or photonic crystal fiber (PCF)[16,17,25,26]. Although the output power and conversion efficiency are desirable by these strategies, the great preparation difficulties originating from such fiber structures hamper the development of such fibers and fiber lasers. Moreover, the low compactness and integration of these setups is another limiting factor in practical applications.

As is well known, all-fiber lasers have unique superiorities in terms of compact structure and excellent laser performance, which greatly promoted their commercial applications. Additionally, they can simultaneously be utilized as the seed source of high-power laser by master-oscillator power-amplifier (MOPA). Recently, Shi *et al.* realized a single-frequency fiber laser at 930 nm based on a Nd^{3+}-doped fiber, which is expected to be the seed source of high-power narrow-linewidth laser for generating blue fiber laser[8]. In this Letter, to investigate whether it can realize an all-fiber laser at shorter

wavelengths (<920 nm) for obtaining fiber laser in the pure blue area, a fiber laser at 915 nm was further explored based on polarization-maintaining (PM) Nd^{3+}-doped silica fiber. The corresponding optical elements at 915 nm, such as fiber Bragg grating (FBG) and wavelength division multiplexer (WDM), were specially customized.

The fiber is a single-mode PM Nd^{3+}-doped silica fiber (Nufern, Inc.). The diameter of the core and cladding is 5/125 μm. Chemical analyses were performed through wavelength-dispersive X-ray fluorescence spectroscopy (WDS) on an electron probe microanalyzer (EPMA-1600, Shimadzu). The output power was measured by a power meter (Ophir NoraII). The laser spectrum was measured by an optical spectrum analyzer (AQ6370C, Yokogawa). The longitudinal-mode properties of the 915 nm fiber laser were measured by using a scanning Fabry–Pérot interferometer (FPI) with a free spectral range (FSR) of 1.5 GHz, a finesse of 200, and a resolution of about 7.5 MHz. All the measurements were performed at room temperature.

The gain coefficient of an active fiber largely determines the laser performance including laser output power and conversion efficiency. To investigate the gain property at 0.9 μm of this silica fiber, the net gain coefficient was measured by the setup illustrated in Fig. 1(a). A 915 nm and an 808 nm LD were chosen as the signal and pump source, which were directly fusion spliced with an 808/900 WDM. The gain fiber length is 4.5 cm and a 915 nm isolator (ISO) was selected to prevent returning light. Another 808/900 WDM was selected to split the signal and residual pump. The net gains versus the pump powers for different signal powers (2.6, 5.6, and 7.8 mW) are depicted in Fig. 1(b). The net gain per unit length

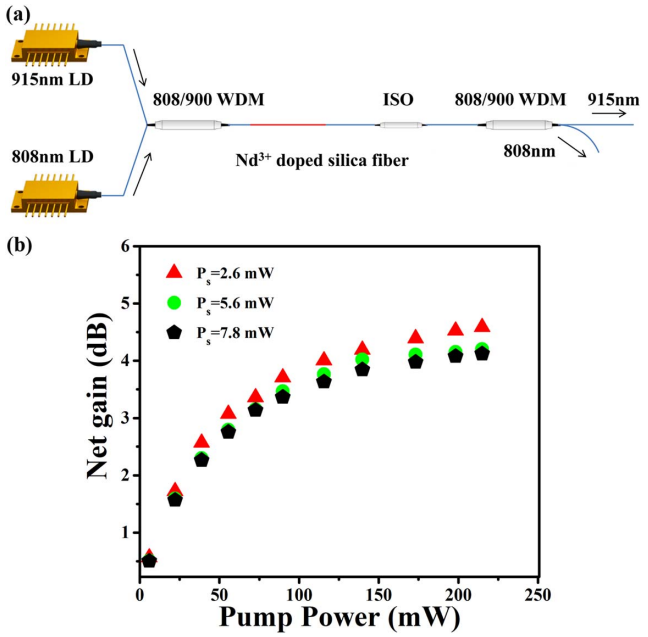

Fig. 1 (a) Setup of the gain coefficient measurement at 915 nm of the Nd^{3+}-doped silica fiber. (b) Net gains versus pump powers of a 4.5 cm Nd^{3+}-doped silica fiber for different signal powers (P_s).

of this Nd^{3+}-doped silica fiber was calculated to be 1.0 dB/cm at 915 nm, which to our best knowledge is the highest gain coefficient reported in this kind of silica fiber. This gain value may be attained by the high doping concentration of Nd^{3+}, which is up to 2.51 wt.% with co-doping the dispersant Al_2O_3, as measured by the WDS. The high gain coefficient is conducive to achieve a high output power and conversion efficiency.

As shown in Fig. 2(a), we further constructed the experimental setup of 915 nm fiber laser. The laser cavity consists of one high-reflection FBG (HR-FBG) and one low-reflection FBG (LR-FBG), which was fused spliced to Nd^{3+}-doped silica fiber. The HR-FBG was imprinted in Hi-780 fiber with a 3 dB linewidth of 0.7 nm and >99% reflectivity at 915 nm. The LR-FBG was fabricated in PM-780 fiber with a 3 dB linewidth of 0.06 nm and 70% reflectivity. Owing to the birefringence of the PM fiber, the reflection spectrum can be created with two different reflection peaks corresponding to two linear polarizations. Only the LR peak along the slow axis overlaps with the

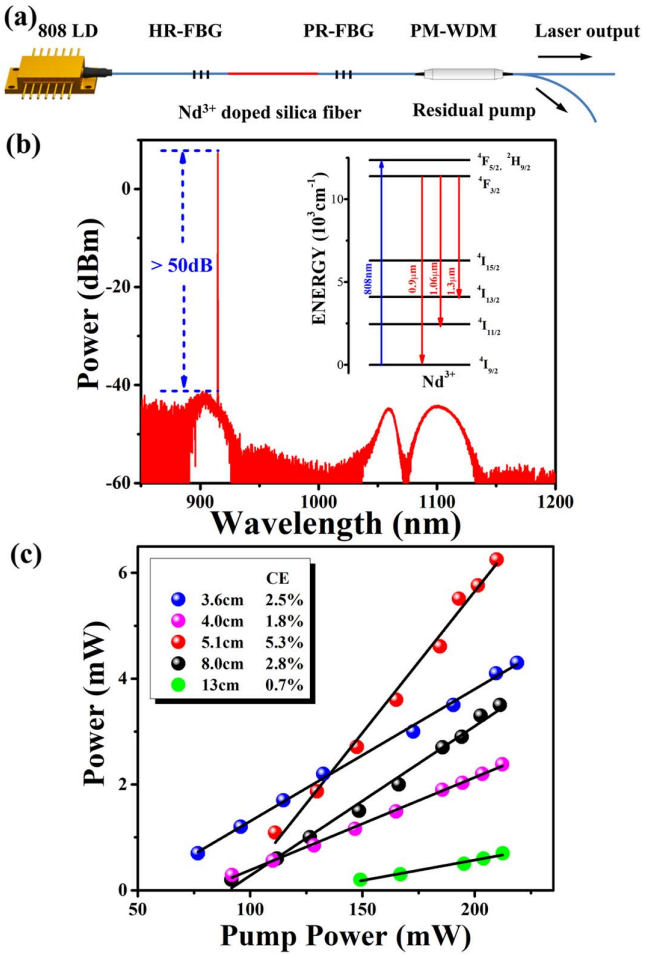

Fig. 2. (a) The experimental setup of 915 nm Nd^{3+}-doped silica fiber laser. (b) 915 nm laser spectrum of Nd^{3+}-doped silica fiber. The inset is the energy level of Nd^{3+}. (c) The laser output power with different lengths of gain fiber versus pump power (CE: optical-to-optical conversion efficiency).

HR peak. A PM-WDM was used to split the residual pump and linearly polarized 915 nm laser output.

Figure 2(b) illustrates the 915 nm laser spectrum under 5.1 cm long silica fiber. Clearly, the 915 nm laser signal can be observed, and there are also strong amplified spontaneous emissions (ASEs) at 1.06 μm and 1.1 μm, which stem from the four-level $^4F_{3/2} \rightarrow {}^4I_{11/2}$ transition. Figure 2(c) illustrates the laser conversion efficiency under different fiber lengths. Since there is no power saturation phenomenon with the increasing pump power, the output power could be further increased. The optical-to-optical efficiency varies with fiber length and presents an optimal value of 5.3% under a 5.1 cm fiber length. This undesirable conversion efficiency is primarily caused by the strong ASE from the four-level transition, which could extract much pump power[27]. Generally, increasing the reflectivity of the output FBG is a feasible method to suppress the strong ASE, yet it also impacts the laser conversion efficiency.

To find the balance between conversion efficiency and the suppression of ASE, the reflectivity of the output FBG with a higher reflectivity of the LR-FBG (83%, 90%) at 915 nm was further selected. Figure 3 depicts the conversion efficiency at a 5.1 cm active fiber length with different LR-FBGs. As is shown, the conversion efficiency decreases significantly from 5.3% to 1.9% with the increasing reflectivity of the FBG to 90%. Thus, for the requirement of high conversion efficiency, the LR-FBG with 70% reflectivity is the best choice of this Nd^{3+}-doped silica fiber in realizing 915 nm all-fiber laser.

Single-frequency fiber lasers have advantages of narrow linewidth, low noise, and large coherence length , presenting wide applications in extensive fields[8,10,27]. Here, we established a distributed Bragg reflector (DBR) structure short cavity to explore the possibility in realizing single-frequency 915 nm fiber laser based on this silica fiber. Considering that the 915 nm laser oscillation cannot be formed due to lack of sufficient gain when the gain fiber length is less than 25 mm, this active fiber length was utilized in the DBR cavity. The HR-FBG and LR-FBG cleaved very close to the grating area are directly spliced to Nd^{3+}-doped silica fiber. At this case, the total length of the DBR cavity is approximately 40 mm considering the effective grating length of HR-FBG and LR-FBG. Figure 4(a) illustrates the laser spectrum with a 0.02 nm optical spectrum analyzer (OSA) resolution, and the exact laser wavelength is 915.34 nm. The inset is the output laser power versus the launched power; the optical-to-optical conversion efficiency is only 0.6% owing to the short gain fiber length. Further, we measured the longitudinal-mode properties by FPI. As illustrated in Fig. 4(b), there are still 6 longitudinal modes in the present cavity. According to the mechanism of single-frequency by a DBR short cavity structure, to meet the requirement of single-frequency operation, the spacing of two adjacent longitudinal modes ($\Delta\nu_q$) must be larger than half of the FWHM of the gain curve($\Delta\nu_{\mathrm{FWHM}}$)[10,27]:

$$\Delta\nu_q > 1/2 \times \Delta\nu_{\mathrm{FWHM}}.$$

At the present cavity length, the $\Delta\nu_q$ is determined to be 2.5 GHz by the equation of $\Delta\nu_q = c/2nL$, where c is the speed of light, n is the refractive index of the core, and L is the length of the cavity. Additionally, the $\Delta\nu_{\mathrm{FWHM}}$ of the gain curve can be determined to be 21 GHz by the equation of $\Delta\nu_{\mathrm{FWHM}} = c\Delta\lambda/\lambda^2$, where $\Delta\lambda$ is the bandwidth of LR-FBG and λ is the laser central wavelength. Obviously, the present conditions still cannot satisfy the single-frequency operation.

The effective approach to reduce the number of longitudinal modes is to shorten the length of the cavity and decrease the $\Delta\nu_{\mathrm{FWHM}}$ of LR-FBG. Considering the unit gain coefficient of this fiber at 915 nm, further shortening the length of gain fiber would lead to no laser oscillation. In order to achieve a single-frequency 915 nm laser output,

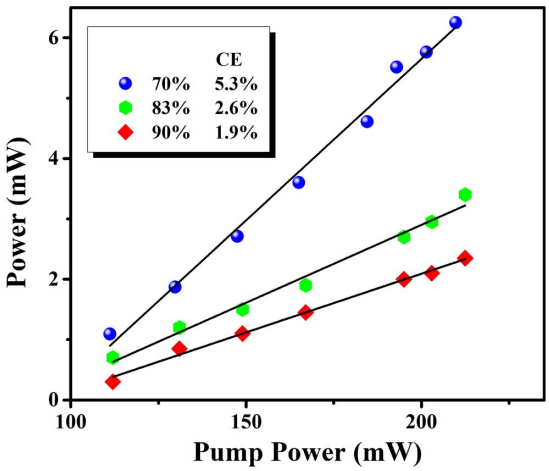

Fig. 3. Dependence of optical-to-optical conversion efficiency on the reflectivity of LR-FBG (70%, 83%, 90%) with a 5.1 cm fiber length.

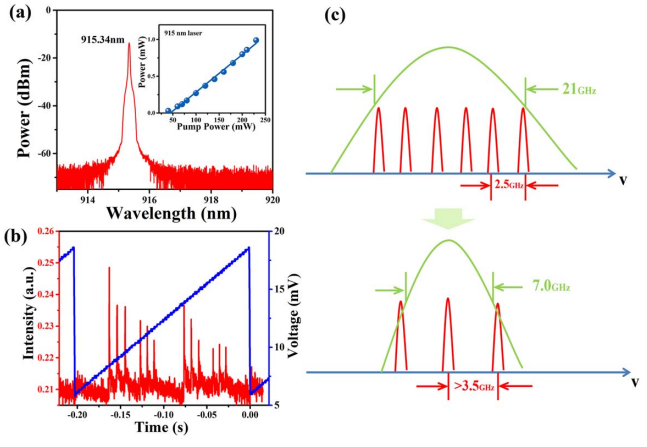

Fig. 4. (a) Laser spectrum with a 0.02 nm OSA resolution. The inset is the output laser power versus the launched pump power. (b) The longitudinal-mode properties of DBR 915 nm fiber laser measured by FPI. (c) A brief schematic diagram of reducing the number of longitudinal modes in the DBR cavity.

if the imprinted overall effective grating length of HR-FBG and LR-FBG can be further shortened to less than 5 mm, the length of the cavity will be reduced to less than 30 mm. As shown in Fig. 4(c), the spacing of adjacent longitudinal modes would increase to more than 3.5 GHz. Meanwhile, if the bandwidth of LR-FBG can be shortened to 0.02 nm, meaning the $\Delta\nu_{\mathrm{FWHM}}$ is 7 GHz, it completely meets the condition of single-frequency operation and could realize the single-frequency 915 nm laser oscillation.

In conclusion, the three-level all-fiber laser at 915 nm based on Nd^{3+}-doped silica fiber under different fiber lengths was realized. The net gain coefficient at 915 nm was measured and calculated to be 1.0 dB/cm . The optical-to-optical conversion efficiency varies with active fiber length and the reflectivity of the output FBG, presenting an optimal value of 5.3% at 5.1 cm fiber length and 70% reflectivity of LR-FBG. In addition, there are still multi-longitudinal modes of laser oscillation under short 40 mm DBR laser cavity. Through further shortening the effective grating length of the pair of silica FBG and decreasing the reflective bandwidth of the LR-FBG, the single-frequency 915 nm laser may be realized. Our results indicate that the PM Nd^{3+}-doped silica fiber could achieve a 915 nm all-fiber laser output, which presents the potential to realize single-frequency 915 nm fiber laser and could be the seed source of high-power fiber laser for realizing pure blue fiber laser.

This work was supported by the National Key Research and Development Plan (No. 2017YFF0104504), Guangdong Natural Science Foundation (No. 2018B030308009), National Natural Science Foundation of China (No. 51672085), Program for Innovative Research Team in University of Ministry of Education of China (No. IRT_17R38), Joint Fund of Ministry of Education of China (No. 6141A02033225), Local Innovative Research Team Project of "Pearl River Talent Plan" (No. 2017BT01X137), Science and Technology Project of Guangdong (No. 2017B090911005), and Guangdong Key R&D Program (No. 2018B090904003).

References

1. M. E. Fermann and I. Hartl, Nat. Photon. **7**, 868 (2013).
2. D. J. Richardson, J. Nilsson, and W. A. Clarkson, J. Opt. Soc. Am. B **27**, B63 (2010).
3. B. Leconte, H. Gilles, T. Robin, B. Cadier, and M. Laroche, Opt. Express **26**, 10000 (2018).
4. Y. Zhang, J. Liu, J. Wu, R. Ma, D. Wang, and J. Zhang, Opt. Express **24**, 19769 (2016).
5. K. Kojima, U. T. Schwarz, M. Funato, Y. Kawakami, S. Nagahama, and T. Mukai, Opt. Express **15**, 7730 (2007).
6. K. Kojima, M. Funato, Y. Kawakami, S. Nagahama, T. Mukai, H. Braun, and U. T. Schwarz, Appl. Phys. Lett. **89**, 241127 (2006).
7. C. Yang, Z. Huang, H. Deng, Q. Zhao, Y. Zhang, J. Gan, H. Cheng, Z. Feng, M. Peng, Z. Yang, and S. Xu, J. Opt. **20**, 025803 (2018).
8. Q. Fang, Y. Xu, S. Fu, and W. Shi, Opt. Lett. **41**, 1829 (2016).
9. A. Bouchier, G. Lucas-Leclin, P. Georges, and J. M. Maillard, Opt. Express **13**, 6974 (2005).
10. Z. Huang, H. Deng, C. Yang, Q. Zhao, Y. Zhang, Y. Zhang, Z. Feng, Z. Yang, M. Peng, and S. Xu, Opt. Express **25**, 1535 (2017).
11. X. Zhu, W. Shi, J. Zong, D. Nguyen, R. A. Norwood, A. Chavez-Pirson, and N. Peyghambarian, Opt. Lett. **37**, 4167 (2012).
12. S. Zheng, J. Li, C. Yu, Q. Zhou, L. Hu, and D. Chen, Ceram. Interfaces **43**, 5837 (2017).
13. Z. Zhang, J. Cao, J. Zheng, M. Peng, S. Xu, and Z. Yang, Chin. Opt. Lett. **15**, 121601 (2017).
14. P. Zheng, S. Li, L. Wang, T.-L. Zhou, S. You, T. Takeda, N. Hirosaki, and R.-J. Xie, ACS Appl. Mater. Interfaces **10**, 14930 (2018).
15. J. Yu, S. Si, Y. Liu, X. Zhang, Y. Cho, Z. Tian, R. Xie, H. Zhang, Y. Li, and J. Wang, J. Mater. Chem. C **6**, 8212 (2018).
16. B. Leconte, B. Cadier, H. Gilles, S. Girard, T. Robin, and M. Laroche, in *Advanced Solid State Lasers*, OSA Technical Digest (online) (2015), paper AW2A.3.
17. I. A. Bufetov, V. V. Dudin, A. V. Shubin, A. K. Senatorov, E. M. Dianov, A. B. Grudinin, S. E. Goncharov, I. D. Zalevskii, A. N. Gur'yanov, M. V. Yashkov, A. A. Umnikov, and N. N. Vechkanov, Quantum Electron. **33**, 1035 (2003).
18. J. Dawson, R. Beach, A. Drobshoff, Z. Liao, D. Pennington, S. Payne, L. Taylor, W. Hackenberg, and D. Bonaccini, in *Advanced Solid-State Photonics*, OSA Technical Digest (2004), paper MD8.
19. W. T. Li, M. Li, J. M. Chen, P. W. Kuan, D. P. Chen, Q. L. Zhou, and L. L. Hu, IEEE Photon. Tech. Lett. **28**, 2295 (2016).
20. Y. Wang, Y. Zhang, J. Cao, L. Wang, X. Peng, J. Zhong, C. Yang, S. Xu, Z. Yang, and M. Peng, Opt. Lett. **44**, 2153 (2019).
21. B. Bai, Y. Bai, D. Li, Y. Sun, J. Li, and J. Bai, Chin. Opt. Lett. **16**, 031402 (2018).
22. S. Han, X. Li, H. Xu, Y. Zhao, H. Yu, H. Zhang, Y. Wu, Z. Wang, X. Hao, and X. Xu, Chin. Opt. Lett. **12**, 011401 (2014).
23. K. Linganna, R. Narro-García, H. Desirena, E. De la Rosa, C. Basavapoornima, V. Venkatramu, and C. K. Jayasankar, J. Alloys Compd. **684**, 322 (2016).
24. Y. Wang, J. Cao, X. Li, J. Li, L. Tan, S. Xu, and M. Peng, J. Am. Ceram. Soc. **102**, 1694 (2019).
25. J. Dawson, A. Drobshoff, Z. Liao, R. Beach, D. Pennington, and S. Payne, Proc. SPIE **4974**, 75 (2003).
26. A. Wang, A. K. George, and J. C. Knight, Opt. Lett. **31**, 1388 (2006).
27. C. Yang, Q. Zhao, Z. Feng, M. Peng, Z. Yang, and S. Xu, Opt. Express **24**, 29795 (2016).